

Split-gasket approach to the integration of electrical leads into diamond anvil cells

Neha Kondedan^a, Ulrich Häussermann^b, and Andreas Rydh^a

^aDepartment of Physics, Stockholm University, SE-10691 Stockholm, Sweden

^bDepartment of Materials and Environmental Chemistry, Stockholm University, SE-10691 Stockholm, Sweden

ARTICLE HISTORY

Compiled February 4, 2025

ABSTRACT

Transport and heat capacity measurements under pressure must reconcile the limited available space and complicated geometry of a high-pressure cell with the need for multiple electrical connections. One solution for diamond anvil cells is to use customized diamonds with deposited electrical leads. Here, we instead address the problem through a split-gasket approach, intended for diamond anvil cells at moderate pressures and low temperature. A key component is the use of a substrate with lithographically defined leads, which enables connections to components such as thermometer, heater, and/or sample within the confined sample volume of the cell. The design includes an elaborate BeCu gasket sandwich with a preparation method that ensures electrical contact integrity. Using this configuration, we bring 12 leads to within $100\ \mu\text{m}$ of the center of the diamond anvil at a pressure of about 2 GPa, comparable to the pressure reached with a regular gasket, demonstrating the setup's capability for high-pressure experiments. The split-gasket approach may come at the cost of reduced maximum pressure, but brings versatility and reproducibility, and alleviates the experimental efforts of maintaining multiple electrical leads both intact and electrically isolated.

KEYWORDS

Diamond Anvil Cell, high pressure, gasket-sandwich, substrate, ruby fluorescence spectrum, PEEK.

1. Introduction

Hydrostatic pressure serves as a tuning parameter in the study of material properties across various condensed matter disciplines [1–5]. Pressure can induce effects similar to chemical doping, without compromising crystal quality, by modifying the lattice parameters [6–8]. The resulting effects on orbital overlap, electronic correlation, and density of states may be profound [9,10]. Consequently, pressure is an extended dimension, in addition to the use of magnetic fields, in the study of electrical resistivity, specific heat, AC susceptibility, and dielectric properties in a range of materials, particularly in superconductors and magnetic systems [11–14]. Variations of the diamond anvil cell (DAC) [15], a successor to Bridgman's opposed anvil cell [16], have been widely used to generate static pressures up to the 100 GPa range and beyond [17–20]. However, the maximum pressure is related to the chamber volume, typically limiting the attainable pressures for setups such as specific heat to the 1 - 20 GPa range [21–26].

A major challenge in conducting high-pressure measurements lies in introducing electrical feedthroughs into the small pressure chamber containing the sample of interest, without causing a short circuit with the gasket, and maintaining stable contacts to the sample under high pressure. Various methods have been employed to achieve reliable electrical connections. For resistivity measurements, there exist setups

Email: neha.kondedan@fysik.su.se

Email: andreas.rydh@fysik.su.se

where four wires are attached to the corners of a sample in a four-probe geometry, using either silver paste [27–29], in-situ soldering [30,31], or mechanical contacts under applied stress [32,33]. For some samples with low adhesion, contact pads are first deposited onto the surface, and the wires are then attached to these pads using silver epoxy [34]. Another way used is to deposit the leads onto the sample itself [35]. Efforts have been made to introduce leads into the sample volume by depositing them onto the diamond anvil culet using sputtering or evaporation techniques [36–39], or by advanced techniques such as 3D laser pantography or 2D projection lithography followed by epitaxial diamond chemical vapor deposition [40].

Beyond resistivity measurements, other setups under high pressure include anomalous Hall conductivity, which is conducted with leads deposited on an insulated gasket [41], ionic conductivity measured with electrodes on the diamond anvil [42], and magnetic susceptibility measurements with specially fabricated leads on the diamond anvil [43]. AC calorimetry measurements require the incorporation of a heater and thermometer near the sample, necessitating at least four incoming leads. There are AC calorimetry setups that utilize insulator gaskets [21–23], and insulated gaskets [24]. Some setups place the heater and thermometer outside the pressure chamber [25,26], but this requires good thermal conduction within the cell, adding to the addenda heat capacity.

To prevent shorts between metallic gaskets and leads, non-metallic gaskets or insulated metallic gaskets are typically used. Non-metallic gaskets, such as amorphous boron [44], boron composites [45], diamond powder-epoxy mixtures [46], have been employed as inserts within metal gaskets or as standalone gaskets. Given the mechanical advantages of metallic gaskets, many experiments utilize insulator-coated metallic gaskets. These include metal gaskets covered with an Al_2O_3 layer [30,33], an Al_2O_3 and NaCl mixture [37], a layer of Al_2O_3 followed by a Kapton foil [38], an Al_2O_3 and epoxy mixture [29,31], mica and MgO powder [47], as well as Zylon fibers with diamond paste [48].

The primary issues with all of these setups and approaches include severing of the electric leads and their insulation by the edges of the diamond or the gasket hole, shorts to the gasket, and loss of contact with the sample under stress. Additionally, making contact with the sample can be challenging, depending on its surface characteristics and geometry. Non-hydrostatic pressure conditions may also fail the contacts during the experiment due to minor movements of the sample within the sample volume. These issues can be addressed by introducing a robust substrate with deposited electrical leads that extends all the way from the center of the pressure chamber to the external connections on the outside. Unlike other setups, this substrate prevents direct contact between the leads and the diamond anvil, reducing the risk of damage due to the diamond edges.

2. Experimental setup

Here, we use a miniature DAC (manufactured at Earth & Planets Laboratory, Carnegie Institution for Science) weighing 39 g, with a diameter of 22 mm and a height of 28 mm, as shown in Figure 1(a). Its small size and low mass facilitate use with various probes and cryogenic systems. A conical aperture, with a diameter of 1 mm at the top of the cylinder, allows for optical viewing and pressure measurements. The diamond anvils are type IIa, 16-sided, with a culet size of 1.2 mm (supplied by Almax easyLab). The piston and cylinder design enables the application of force, which is employed by turning the four screws on top of the cell and regulated by the spring to achieve a uniform distribution of force. The top diamond is affixed to the cylinder and the bottom diamond to the piston, using Stycast 2850FT epoxy and working under optical stereoscope and viewing through the top diamond. The cell body is made of steel and some parts of BeCu (98% Cu - 2% Be).

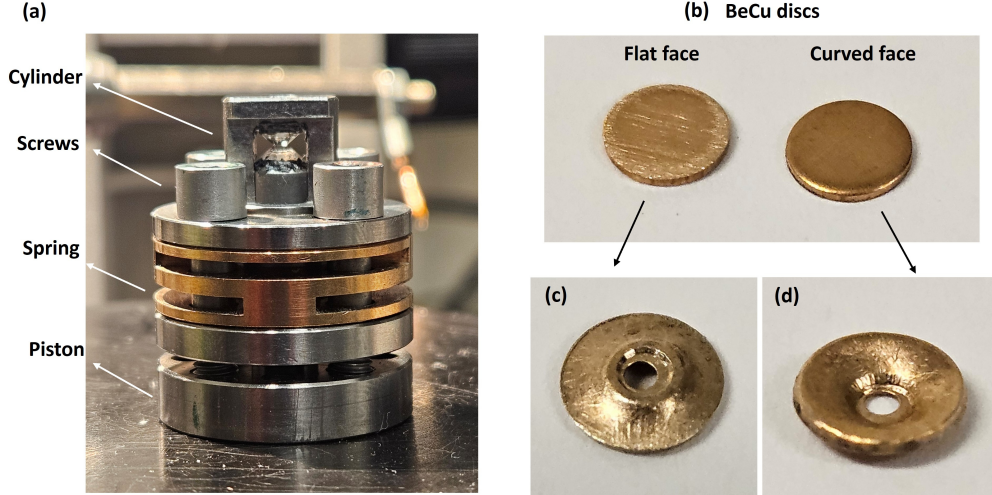


Figure 1. (a) Miniature diamond anvil cell with 28 mm height and 22 mm diameter. (b) BeCu discs of 4 mm diameter and 380 μm thickness, used as top gasket before indentation. The flat/curved asymmetry of the faces arises from the gasket punching process, used here to control the cupping direction of the gaskets. (c) Flat side of the disc after pre-indenting. (d) Curved side after pre-indenting. It is cupped as a girdle around the top anvil due to the initial curvature of the face.

3. Preparation of gaskets

The split-gasket approach requires a thicker gasket beneath the top diamond and a thinner gasket on the bottom diamond. We use BeCu as the gasket material, as it performs well across a wide range of temperatures, particularly at low temperatures, due to its excellent mechanical properties and minimal magnetic background [49]. A BeCu disc with a thickness of 380 μm and a diameter of 4 mm is used as the upper gasket material, which is indented to achieve the optimal final thickness. This punched disc features two asymmetric faces — one flat and one with curved edges, as illustrated in Figure 1(b). This asymmetry is critical for the setup. The indentation on one side leaves the opposite side flat, allowing it to face the substrate and preventing excessive deformation under pressure. For pre-indentation and hole drilling, first the BeCu disc is pre-indenting to a thickness of approximately 230 μm . This process causes one face to remain flat, while the gasket cups toward the curved face, as shown in Figure 1(c) and (d), respectively. Second, a 600 μm pilot hole is drilled at the center of the disc using electrical discharge machining. The disc is then indented further, causing additional deformation and a reduction in the hole size. This step is essential to prevent the pressure chamber from shrinking during the experiment. The additional indentation reduces the central thickness to approximately 130 μm and decreases the hole size to around 400 μm . The hole is then redrilled to restore its original size. The surface roughness of the disc is measured by averaging the profile deviations from a scan conducted using a Stylus Profilometer KLA Tencor P7. After machining, the roughness is approximately 0.5 μm , indicating a relatively smooth surface.

The lower gasket is a 50 μm thick BeCu foil. This gasket is typically cut to match the size of the electrical leads substrate, primarily serving as support for the substrate. Due to its small thickness compared to the top gasket, the lower gasket exhibits minimal deformation under applied force [50]. Therefore, it does not require pre-indentation. The surface roughness of the foil is about 0.3 μm . Both gaskets are uninsulated.

4. Integrating leads into the cell

The electrical leads are integrated through a thin, electrically insulating substrate with lithographically patterned leads. The leads' design allows multiple leads to be positioned close to the sample inside the

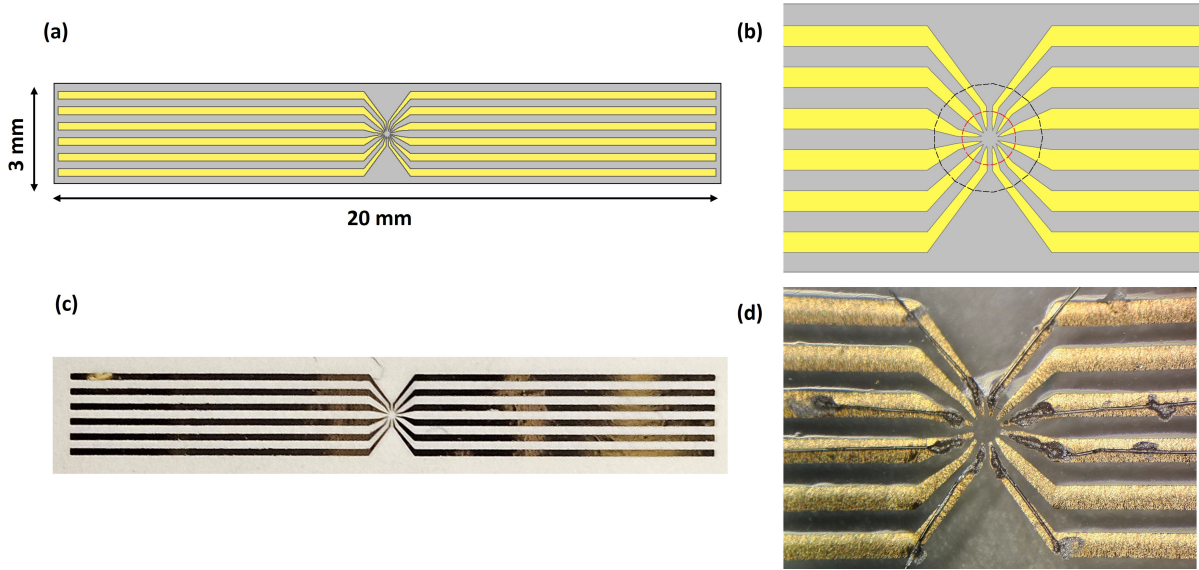


Figure 2. (a) Layout of the substrate with metallic leads on top. (b) Magnified view of the center of the substrate where the leads converge to a circle, on top of which a sample or wafer chip can be attached. The locations of the diamond culet edges (black line) as well as the gasket hole (red line) are indicated by dashed lines. (c) PEEK substrate with deposited Cr+Au leads. (d) Central area with small pieces of Al wires attached to the leads, to reinforce the electrical contacts where most part of the deformation takes place under pressure.

sample volume. The layout of the substrate with leads is shown in Figure 2(a). With a length of 20 mm, the substrate extends outside the chamber to make external connections. The design incorporates 12 leads arranged in a circular pattern at the center, with a diameter of $190\ \mu\text{m}$, as illustrated in Figure 2(b). Each lead has a width of $230\ \mu\text{m}$, gradually narrowing to $10\ \mu\text{m}$ at the center of the circle. These leads are fabricated using nanofabrication techniques.

A non-metallic substrate material, PEEK (Polyether ether ketone), was selected for its excellent chemical, mechanical, and thermal resistance properties under high-pressure conditions. This thermoplastic polymer, with a thickness of $25\ \mu\text{m}$, is a smooth and transparent film compatible with high-vacuum environment and lithography chemistry. The electric leads are fabricated using a combination of photolithography, O_2 plasma ashing, e-beam evaporation, and lift-off techniques. A layer of 30 nm chromium, followed by 50 nm of gold is deposited as the metal leads. Additional thickness can be added, but care should be taken to avoid excessive heating of the PEEK. The resistance of the resulting leads is approximately $6\ \Omega$. Around 20 substrate samples of the required size can be fabricated simultaneously with a 4" wafer system. Figure 2(c) shows a PEEK substrate with the leads after deposition. Small strips of aluminum wires with a diameter of $25\ \mu\text{m}$ are attached to these leads, strengthening the points where the diamond edges meet as well as at the edge of the drilled gasket, to prevent any rupture of the leads under stress, see Figure 2(d).

5. Sample mounting

For resistivity measurements, the sample can be directly attached to the center of the substrate, with electrical contacts for a four-probe geometry or multiterminal setups made to the sample using a two-component silver epoxy (EPO-TEK[®] H20E), which is cured at 125°C for 10 to 15 minutes. Alternatively, a silicon chip that is $30\ \mu\text{m}$ thick and $300\ \mu\text{m}$ in diameter, with deposited leads designed for resistivity measurements, shown in Figure 3(a), can be attached to the center of the substrate using crystal bond. To avoid electrical shorts, the edges of the chip need to be protected by the crystal bond. The electric leads on the substrate can then be connected to the leads on the chip using silver epoxy. The sample is finally

mounted on top of the chip, allowing connections to be made to the sample.

Specific heat measurements require similar preparations. The cell fits a calorimeter chip of a size similar to the silicon chip (30 μm thick and 300 μm in diameter), containing thermometer and heaters. The development of such a calorimeter chip is reported in [51]. The connections are made with silver epoxy as illustrated in Figure 3(b). The sample is secured to the calorimeter surface using a thin layer of Apiezon-N grease or melted crystal bond.

6. Application of pressure

The assembly of the pressure cell components is illustrated in the schematic of Figure 3(e). The electrical leads substrate is placed onto the lower gasket of a similar size, with the sample space positioned at the center of the culet. Some ruby crystals are placed close to the sample to measure the pressure inside the chamber using the ruby fluorescence spectroscopy technique [52]. The sample is then covered by a droplet of liquid pressure medium, which is used to maintain hydrostatic conditions. The liquid medium causes less motion and damage to single crystal samples during the loading, compared to a solid pressure medium. With this setup, we have used Apiezon-N grease and silicone oil, but glycerol or other liquid pressure media should also work.

A 25 μm thick layer of PEEK is placed on top of the leads and sample assembly as an insulation layer to prevent shorts between the upper gasket and the substrate leads. This method of incorporating a separate insulation layer ensures that any plastic deformation in the upper gasket does not directly impact the components beneath it. The transparent PEEK also allows for easier alignment of the upper gasket.

For the alignment of the indented upper gasket with the sample space, some melted crystal bond is first applied to the flat side of the gasket prior to attaching it to the PEEK. This effectively seals any gaps between the gasket and the PEEK, preventing subsequent leakage of pressure medium contained within the gasket hole. When filling the medium, it is necessary to ensure that there are no bubbles, as they can cause volume collapse of the chamber. Once the medium is filled, the properly aligned assembly can be closed with the top diamond anvil, while checking the alignment through the optical window on top of the pressure cell.

Figure 3(f) shows a diagram of the gasket assembly after pressurization. The PEEK insulation effectively acts as part of the pressure medium as long as the chamber is filled and uniformly pressurized. The maximum pressure of about 2 GPa for the culet size used can be achieved without compromising the contacts. Hydrostatic conditions are indicated by the non-broadening of the ruby fluorescence spectral lines, shown in Fig. 3(c). The external leads are subsequently connected to the bonding pads shown in Figure 3(d).

7. Discussion

The described sandwich approach presents a method of pressurizing samples while incorporating electric leads. While other methods may likely reach higher pressures, the split gasket enables various measurements without the need to change most of its components. Swapping the transport or calorimeter chip, replacing the sample, and making new connections with silver epoxy are sufficient to prepare for a new measurement. The upper and lower gaskets, along with the substrate containing the leads, are reusable until they either break or undergo significant deformation. Additionally, this setup accommodates different culet sizes; the same substrate can be utilized with minor modifications to the dimensions of the upper gasket hole. The substrate can easily accommodate larger wafer chips and/or samples.

The process of fabricating the substrate with leads is quite simple, making it easy to alter the lead patterns as needed. With multiple leads available within the pressure chamber, some leads can be reconfigured into a heater, allowing for local Joule heating of the sample. This prevents undesired pressure changes due

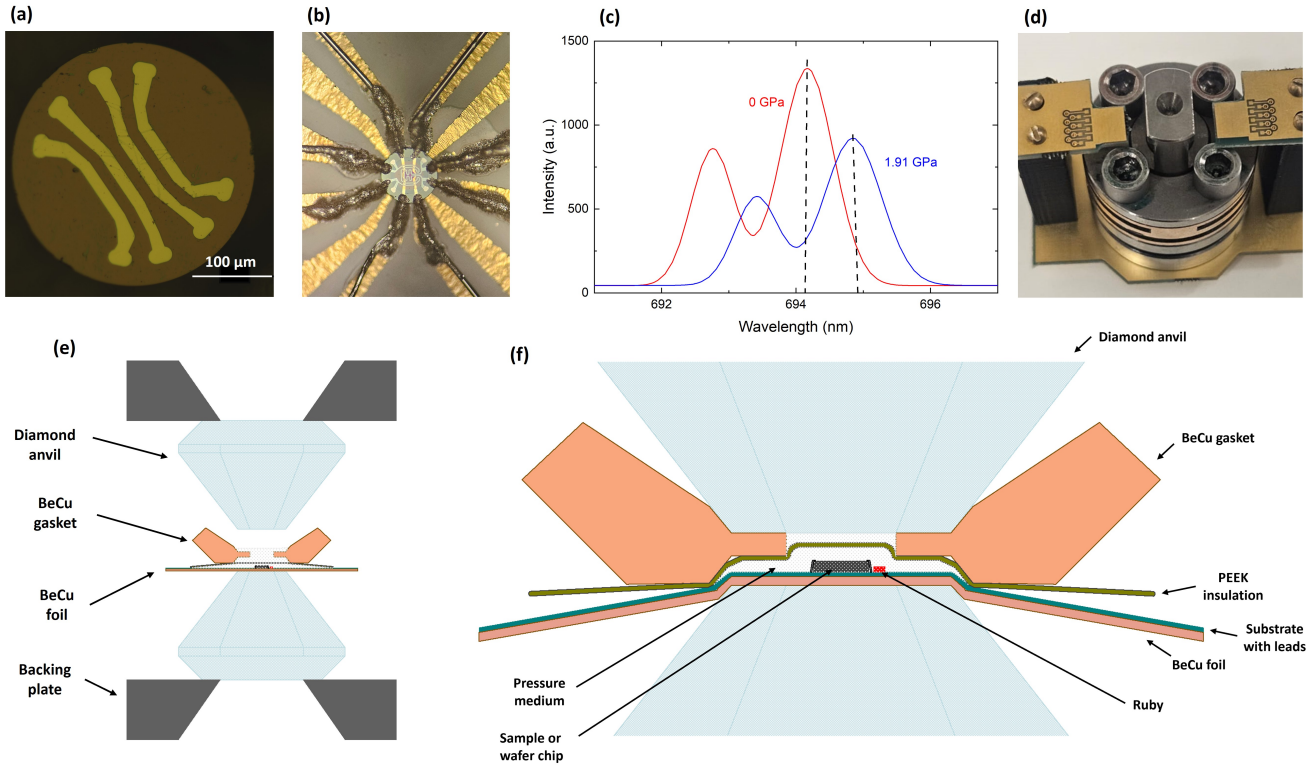


Figure 3. (a) Microscopic image of a Si chip with metal leads for transport measurements, matching the dimensions of the pressure chamber. (b) Miniaturized calorimeter attached to the center of the substrate and connected to the leads using silver epoxy. (c) Ruby fluorescence spectra showing the wavelength shift with pressure, going from 694.16 nm at 0 GPa to 694.85 nm at 1.91 GPa. (d) Bonding pads for the external electrical attachment of the substrate outside the DAC, allowing the lead ends to connect via wire bonding. (e) Schematic showing the gasket-sandwich before applying pressure. (f) Diagram showing the deformation of the gasket-sandwich components after the application of pressure.

to temperature changes of the DAC arising from thermal expansion effects, if working at low temperature.

8. Conclusions

In conclusion, we have developed a high-pressure setup that can be used for various transport and calorimetry measurements requiring several electrical leads (12 demonstrated here). The key components of this approach include a split gasket and an insulating substrate with integrated leads. We find that the split-gasket solution is not limiting the pressure range of the cell that we use, reaching about 2 GPa with a 1.2 mm culet size without damaging the leads. The ease of modifying and reproducing the pressure cell components makes this setup versatile for modest pressure experiments. There is potential to reach even higher pressures by modifying the culet size and sample volume. Whether the split gasket design will limit the ultimate pressure in such a case remains to be investigated.

Acknowledgements

Support from the Knut and Alice Wallenberg Foundation under Grant No. KAW 2018.0019 and the Swedish Research Council, Grant No. 2021-04360, are acknowledged. We thank P. Lazor for fruitful discussions and H. Breton for introduction to the pressure cell operation.

References

- [1] Khasanov R, Sanna S, Prando G, Shermadini Z, Bendele M, Amato A, Carretta P, De Renzi R, Karpinski J, Katrych S, and Luetkens H. Tuning of competing magnetic and superconducting phase volumes in $\text{LaFeAsO}_{0.945}\text{F}_{0.055}$ by hydrostatic pressure. *Phys. Rev. B.* 2011;84:100501.
- [2] Gati E, Köhler S, Guterding D, Wolf B, Knöner S, Ran S, Bud'ko SL, Canfield PC, and Lang M. Hydrostatic-pressure tuning of magnetic, nonmagnetic, and superconducting states in annealed $\text{Ca}(\text{Fe}_{1-x}\text{Co}_x)_2\text{As}_2$. *Phys. Rev. B.* 2012;86:220511.
- [3] Wu W, McCollam A, Grigera SA, Perry RS, Mackenzie AP, and Julian SR. Quantum critical metamagnetism of $\text{Sr}_3\text{Ru}_2\text{O}_7$ under hydrostatic pressure. *Phys. Rev. B.* 2011;83:045106.
- [4] Zhang Z, Shao J, Jin F, Dai K, Li J, Lan D, Hua E, Han Y, Wei L, Cheng F, and Ge B. Uniaxial strain and hydrostatic pressure engineering of the hidden magnetism in $\text{La}_{1-x}\text{Ca}_x\text{MnO}_3$ ($0 \leq x \leq 1/2$) thin films. *Nano Letters.* 2022;22:7328-7335.
- [5] Ponkratz U, Nicula R, Jianu A, and Burkel E. Quasicrystals under pressure: a comparison between Ti-Zr-Ni and Al-Cu-Fe icosahedral phases. *Journal of Non-Crystalline Solids.* 1999;250:844-848.
- [6] Gati E, Xiang L, Bud'ko SL, and Canfield PC. Hydrostatic and uniaxial pressure tuning of iron-based superconductors: Insights into superconductivity, magnetism, nematicity, and collapsed tetragonal transitions. *Annalen der Physik.* 2020;532:2000248.
- [7] Lü X, Yang W, Quan Z, Lin T, Bai L, Wang L, Huang F, and Zhao Y. Enhanced electron transport in Nb-doped TiO_2 nanoparticles via pressure-induced phase transitions. *JACS.* 2014;136:419-426.
- [8] Moritomo Y, Asamitsu A, and Tokura Y. Pressure effect on the double-exchange ferromagnet $\text{La}_{1-x}\text{Sr}_x\text{MnO}_3$ ($0.15 \leq x \leq 0.5$). *Phys. Rev. B.* 1995;51:16491.
- [9] Hemley RJ and Ashcroft NW. The revealing role of pressure in the condensed matter sciences. *Physics Today.* 1998;51:26-32.
- [10] Mao HK, Chen B, Chen J, Li K, Lin JF, Yang W, and Zheng H. Recent advances in high-pressure science and technology. *Matter and Radiation at Extremes.* 2016;1:59-75.
- [11] Wang X and Kamenev KV. Review of modern instrumentation for magnetic measurements at high pressure and low temperature. *Low Temperature Physics.* 2014;40:735-746.
- [12] Flores-Livas JA, Boeri L, Sanna A, Profeta G, Arita R, and Eremets M. A perspective on conventional high-temperature superconductors at high pressure: Methods and materials. *Physics Reports.* 2020;856:1-78.
- [13] Gor'kov LP and Kresin VZ. Colloquium: High pressure and the road to room temperature superconductivity. *Rev. Mod. Phys.* 2018;90:011001.
- [14] Woollam JA and Chu CW. High-pressure and low-temperature physics. Springer Science & Business Media; 2012 Dec 6.
- [15] Jayaraman A. Diamond anvil cell and high-pressure physical investigations. *Rev. Mod. Phys.* 1983;55(1):65.
- [16] Bridgman PW. The resistance of 72 elements, alloys, and compounds to $100,000 \text{ kg/cm}^2$. In: *Papers 169-199.* Harvard University Press; 1964:4113-4197.
- [17] Dubrovinsky LS, Saxena SK, Tutti F, Rekhii S, and LeBehan T. In situ X-ray study of thermal expansion and phase transition of iron at multimegabar pressure. *Phys. Rev. Lett.* 2000;84(8):1720.
- [18] Dubrovinsky L, Dubrivinskaia N, Prakapenaka VB, and Abakumov AM. Implementation of micro-ball nanodiamond anvils for high-pressure studies above 6 Mbar. *Nature commun.* 2012;3:1163.
- [19] Drozdov AP, Eremets MI, Troyan IA, Ksenofontov V, and Shylin SI. Conventional superconductivity at 203 kelvin at high pressures in the sulfur hydride system. *Nature.* 2015;525(7567):73-6.
- [20] Yagi T, Sakai T, Kadobayashi H, and Irifune T. High pressure generation techniques beyond the limit of conventional diamond anvils. *High Pressure Research.* 2020;40(1):148-61.
- [21] Wilhelm H. AC-calorimetry at high pressure and low temperature. *Advances in Solid State Physics.* 2003;889-913.
- [22] Geballe ZM and Struzhkin VV. AC calorimetry of H_2O at pressures up to 9 GPa in diamond anvil cells. *Journal of Applied Physics.* 2017;121(24).
- [23] Lortz R, Junod A, Jaccard D, Wang Y, Meingast C, Masui T, and Tajima S. Evolution of the specific-heat anomaly of the high-temperature superconductor $\text{YBa}_2\text{Cu}_3\text{O}_7$ under the influence of doping through application of pressure up to 10 GPa. *Journal of Physics: Condensed Matter.* 2005;17(26):4135.
- [24] Dasenbrock-Gammon N, McBride R, Yoo G, Dissanayake S, and Dias R. Second harmonic AC calorimetry technique within a diamond anvil cell. *Rev. Sci. Instrum.* 2022;93(9).

- [25] Umeo K. Alternating current calorimeter for specific heat capacity measurements at temperatures below 10 K and pressures up to 10 GPa. *Rev. Sci. Instrum.* 2016;87(6).
- [26] Kubo H, Umeo K, and Takabatake T. Specific-Heat Measurement above 3 GPa using a Bridgman Anvil Cell. *Journal of the Physical Society of Japan.* 2007;76(Suppl. A):221-2.
- [27] Cui C, Tyson TA, Zhong Z, Carlo JP, and Qin Y. Effects of pressure on electron transport and atomic structure of manganites: Low to high pressure regimes. *Phys. Rev. B.* 2003;67(10):104107.
- [28] Colombier E, Torikachvili MS, Ni N, Thaler A, Bud'ko SL, and Canfield PC. Electrical transport measurements under pressure for BaFe₂As₂ compounds doped with Co, Cr, or Sn. *Supercond. Sci. Tech.* 2010;23(5):054003.
- [29] Thomasson J, Dumont Y, Griveau JC, and Ayache C. Transport measurements at low temperatures in a diamond anvil cell with helium as pressure medium. *Rev. Sci. Instrum.* 1997;68(3):1514-7.
- [30] Gonzalez J, Besson JM, and Weill G. Electrical transport measurements in a gasketed diamond anvil cell up to 18 GPa. *Rev. Sci. Instrum.* 1986;57(1):106-7.
- [31] Jaramillo R, Feng Y, and Rosenbaum TF. Four-probe electrical measurements with a liquid pressure medium in a diamond anvil cell. *Rev. Sci. Instrum.* 2012;83(10).
- [32] Torikachvili MS, Bud'ko SL, Ni N, Canfield PC, and Hannahs ST. Effect of pressure on transport and magnetotransport properties in CaFe₂As₂ single crystals. *Phys. Rev. B.* 2009;80(1):014521.
- [33] Erskine D, Yu PY, and Martinez G. Technique for high-pressure electrical conductivity measurement in diamond anvil cells at cryogenic temperatures. *Rev. Sci. Instrum.* 1987;58(3):406-11.
- [34] Patel D and Spain IL. Electrical contact to semiconducting samples for use in the diamond-anvil cell. *Rev. Sci. Instrum.* 1987;58(7):1317-9.
- [35] Leong D, Feyrit H, Prins AD, Wilkinson VA, Homewood KP, and Dunstan DJ. Laminated gaskets for absorption and electrical measurements in the diamond anvil cell. *Rev. Sci. Instrum.* 1992;63(12):5760-3.
- [36] Grzybowski TA and Ruoff AL. Band-overlap metallization of BaTe. *Phys. Rev. Lett.* 1984;53(5):489.
- [37] Straaten JV and Silvera IF. Electrical resistance measurements on cryocrystals in a diamond-anvil cell to 70 GPa. *Rev. Sci. Instrum.* 1987;58(6):994-6.
- [38] Hemmes H, Driessen A, Kos J, Mul FA, Griessen R, Caro J, and Radelaar S. Synthesis of metal hydrides and in situ resistance measurements in a high-pressure diamond anvil cell. *Rev. Sci. Instrum.* 1989;60(3):474-80.
- [39] Gao C, Han Y, Ma Y, White A, Liu H, Luo J, Li M, He C, Hao A, Huang X, and Pan Y. Accurate measurements of high pressure resistivity in a diamond anvil cell. *Rev. Sci. Instrum.* 2005;76(8).
- [40] Weir ST, Akella J, Aracne-Ruddle C, Yogesh KV, and Shane AC. Epitaxial diamond encapsulation of metal microprobes for high pressure experiments. *Applied Physics Letters.* 2000;77(21):3400-3402.
- [41] Wang X, Li Z, Zhang M, Hou T, Zhao J, Li L, Rahman A, Xu Z, Gong J, Chi Z, and Dai R. Pressure-induced modification of the anomalous Hall effect in layered Fe₃GeTe₂. *Phys. Rev. B.* 2019;100(1):014407.
- [42] Wang Q, Liu C, Han Y, Gao C, and Ma Y. The determination of ionic transport properties at high pressures in a diamond anvil cell. *Rev. Sci. Instrum.* 2016;87(12).
- [43] Jackson DD, Aracne-Ruddle C, Malba V, Weir ST, Catledge SA, and Vohra YK. Magnetic susceptibility measurements at high pressure using designer diamond anvils. *Rev. Sci. Instrum.* 2003;74(4):2467-71.
- [44] Lin JF, Shu J, Mao HK, Hemley RJ, and Shen G. Amorphous boron gasket in diamond anvil cell research. *Rev. Sci. Instrum.* 2003;74(11):4732-6.
- [45] Rosa AD, Merkulova M, Garbarino G, Svitlyk V, Jacobs J, Sahle CJ, Mathon O, Munoz M, and Merkel S. Amorphous boron composite gaskets for in situ high-pressure and high-temperature studies. *High Pressure Research.* 2016;36(4):564-74.
- [46] Graf DE, Stillwell RL, Purcell KM, and Tozer SW. Nonmetallic gasket and miniature plastic turnbuckle diamond anvil cell for pulsed magnetic field studies at cryogenic temperatures. *High Pressure Research.* 2011;31(4):533-43.
- [47] Reichlin RL. Measuring the electrical resistance of metals to 40 GPa in the diamond-anvil cell. *Rev. Sci. Instrum.* 1983;54(12):1674-7.
- [48] Yomo S and Tozer SW. Moissanite-anvil cells for the electrical transport measurements at low temperatures. *InJournal of Physics: Conference Series* 2010;215(1):012181. IOP Publishing.
- [49] Heller, Wolfram. Copper-beryllium alloys for technical applications. No. CERN-76-01. European Organization for Nuclear Research, 1976.
- [50] Timofeev YA and Utyuzh AN. Measuring the thickness of a metal gasket squeezed between the anvils of a high-pressure cell while preparing it for an experiment. *Instruments and Experimental Techniques.* 2003;46:721-723.
- [51] Kondedan N and Rydh A. Miniaturized chip calorimeter for high-pressure cells at low temperature. *arXiv preprint arXiv:2501.17659.*

- [52] Chijioke AD, Nellis WJ, Soldatov A, and Silvera IF. The ruby pressure standard to 150GPa. *Journal of Applied Physics*. 2005;98(11).